HHS Public Access

Author manuscript

Neuropharmacology. Author manuscript; available in PMC 2020 October 01.

Published in final edited form as:

Neuropharmacology. 2019 October ; 157: 107666. doi:10.1016/j.neuropharm.2019.107666.

The role of the neuropeptide PEN receptor, GPR83, in the reward pathway: relationship to sex-differences.

Amanda K. Fakira, PhD[1], **Emily G. Peck, BS**[4], **Yutong Liu, MD,PhD**[1,2], **Lindsay M. Lueptow, PhD**[1], **Nikita A. Trimbake, MS**[1], **Ming-Hu Han, PhD**[1,2], **Erin S. Calipari, PhD**[3], **Lakshmi A. Devi, PhD**[1,2]

[1]Department of Pharmacological Sciences, Icahn School of Medicine at Mount Sinai, NY, NY, USA

[2]Nash Family Department of Neuroscience and Friedman Brain Institute, Icahn School of Medicine at Mount Sinai, NY, NY, USA

[3]Department of Pharmacology, Vanderbilt Center for Addiction Research, Vanderbilt Brain Institute, Vanderbilt University School of Medicine, Nashville, TN, USA

[4]Department of Physiology and Pharmacology, Wake Forest School of Medicine, Winston-Salem NC, USA

Abstract

GPR83, the receptor for the neuropeptide PEN, exhibits high expression in the nucleus accumbens of the human and rodent brain, suggesting that it plays a role in modulating the mesolimbic reward pathway. However, the cell-type specific expression of GPR83, its functional impact in the reward pathway, and in drug reward-learning has not been fully explored. Using GPR83/eGFP mice, we show high GPR83 expression on cholinergic interneurons in the nucleus accumbens and moderate expression on ventral tegmental area dopamine neurons. In GPR83 knockout mice, baseline dopamine release in the nucleus accumbens is enhanced which disrupts the ratio of tonic vs phasic release. Additionally, GPR83 knockout leads to changes in the expression of dopamine-related genes. Using the morphine conditioned place preference model, we identify sex differences in morphine reward-learning, show that GPR83 is upregulated in the nucleus accumbens following morphine conditioned place preference, and show that shRNA-mediated knockdown of GPR83 in the nucleus accumbens leads to attenuation morphine reward. Together, these findings detect GPR83 expression in the reward-pathway, and show its involvement in dopamine release and morphine reward-learning.

Keywords

GIR; morphine; proSAAS; voltammetry; cholinergic interneurons; dopamine

Corresponding Author: Dr. Lakshmi A. Devi, PhD, Department of Pharmacological Sciences, Icahn School of Medicine at Mount Sinai, Lakshmi.devi@mssm.edu, Office: 212-241-8345, Lab: 212-241-6545.

1.0 Introduction

G-protein coupled receptors (GPCR) represent a significant portion of marketed pharmaceutical targets; therefore examination of understudied GPCRs may lead to identification of new potential therapeutics. The neuropeptide PEN, derived from the precursor proSAAS, was identified as an endogenous ligand for GPR83 (Gomes et al., 2016). The pattern of GPR83 expression in the brain is similar between mouse, rat and human (Brezillon et al., 2001; Lueptow et al., 2018; Pesini et al., 1998; Sah et al., 2007) with both PEN binding and GPR83 expression being highest in the striatum (Gomes et al., 2016; Müller et al., 2013). Furthermore, GPR83 expression is strongest in the nucleus accumbens (NAc) compared to the dorsal striatum (Pesini et al., 1998).

The strong expression of GPR83 in the NAc suggests that this receptor potentially impacts reward learning, which is encoded by phasic increases in dopamine release from neurons originating in the VTA. Drugs of abuse such as morphine, cocaine and amphetamine cause a phasic release of dopamine in the NAc via actions within the VTA-NAc pathway. *A recent study showed that proSAAS peptides, including the GPR83 ligand PEN, are decreased in the ventral tegmental area (VTA) and NAc following cocaine administration, and that proSAAS knockout mice have deficits in cocaine and amphetamine-induced locomotor sensitization* (Berezniuk et al., 2017). Regarding GPR83, one study showed that its expression is regulated by amphetamine (Wang et al., 2001); however, this study did not investigate the functional impact of the receptor on reward-behaviors. Furthermore, *stress-responses have a critical relationship with the reward system (*Koob and Kreek, 2007; Koob, 2008*), and GPR83 was first described as the glucocorticoid induced receptor (*Harrigan et al., 1989; M T Harrigan et al., 1991*) suggesting that it could play a role in stress responses*. Therefore, although there is evidence of strong GPR83 expression in the NAc and that the PEN-GPR83 receptor system is regulated by drugs of abuse, not much is known about the cell types that express GPR83, as well as the impact of this receptor on reward behaviors and on the dopamine signal responsible for reward-learning.

To address these questions, we utilized a combination of neuroanatomy, physiology and behavioral assays. We used GPR83/eGFP mice to examine the cell type specific expression of GPR83 in the NAc and VTA, fast-scanning cyclic voltammetry (FSCV) to examine the role of GPR83 in dopamine release, and a morphine conditioned place preference (CPP) model, where preference levels are a measure of the rewarding properties of morphine, to investigate the role of GPR83 in reward-learning in male and female mice. We also examined the effect of morphine CPP on GPR83 expression and used lentiviral GPR83 shRNA to examine the effect of GPR83 knockdown in the NAc on morphine CPP. These studies suggest that GPR83 in the NAc plays a role in reward-learning that may involve modulation of dopamine release in this brain region.

2.0 Methods and Materials

2.1 Animals

GPR83/eGFP (Rockefeller University, NY,NY), GPR83 KO and C57BL/6J (Jackson Labs, Bar Harbor ME) male and female mice (8–12 weeks) were maintained on a 12hr light/dark cycle with water and food ad libitum. GPR83/eGFP BAC transgenic mice were generated by the GENSAT project at Rockefeller University. The coding sequence for enhanced green fluorescent protein (eGFP) followed by a polyadenylation signal was inserted into a bacterial artificial chromosome (BAC) at the ATG transcription codon of GPR83. Therefore, cells that express GPR83 mRNA also express eGFP. GPR83 knockout (Jackson Labs, *Bar Harbor, ME*) mice were generated previously (Lu et al., 2007) and *shown to lack GPR83 protein (*Gomes et al., 2016*). Quantitative qPCR analysis confirms that GPR83 KO mice do not express GPR83 mRNA (*Supplemental Figure 1*).* Animal protocols were approved by the IACUC at Icahn School of Medicine at Mount Sinai, according to NIH's Guide for the Care and Use of Laboratory Animals.

2.2 Immunofluorescence and Confocal Imaging

GPR83/eGFP mice were injected with colchicine (75μg/kg), an axonal transport blocker, to visualize dynorphin in neuronal cell bodies, and immunofluorescence studies were performed. Twenty-four to 48 hours after injection of colchicine, mice were perfused with 4% paraformaldehyde in phosphate buffered saline (PBS) pH 7.4 (PFA in PBS). *The brains were removed and post fixed in 4% PFA in PBS overnight. Brains were rinsed 3 times in PBS and* 50 μM coronal brain slices were obtained using a vibratome, *without embedding* the tissue (Leica VT1000, *Buffalo Grove, Il*). To visually enhance eGFP expression, immunohistochemical analysis was carried out using chicken anti-GFP (1:1000) as the primary antibody (Aves Labs, Tigard, OR) and anti-chicken 488 (1:1000) as the secondary *antibody* (Molecular Probes, Eugene, OR). In addition, brain slices were co-stained for dynorphin (1:500; Pen-labs, San Carlos, CA), dopamine- and cAMP-regulated phosphoprotein 32 kDa (1:500; Millipore, *Burlington, MA*), choline acetyl transferase (1:100; Millipore, *Burlington, MA*) or tyrosine hydroxylase (TH; 1:500, Millipore, *Burlington, MA*) overnight followed by anti-goat 594 (1:500) or anti-rabbit 594 (1:500; Molecular Probes, Eugene, OR) secondary antibodies. For TH experiments, anti-sheep 568 (1:500) or anti-sheep 680 (1:500) secondary antibodies were used (Molecular Probes, Eugene, OR). Confocal microscopy was performed in the Microscopy CoRE at the Icahn School of Medicine at Mount Sinai. Confocal z-stack images were taken on a Leica SP5 DMI microscope and processed using Leica software (Leica, *Buffalo Grove, Il).* Secondary antibodies tagged with either 568nm or 680nm *fluorophores* were used to confirm that colocalization was not due to bleed through between the 488nm and 568nm *fluorophores*. To further ensure that co-localization is not due to bleed through, a narrow bandwidth of 498–520nm in the Alexa 488 channel and 570–620nm in the Alexa 568 and 594 channels was used. Co-localization analysis was performed using ImageJ software (*NIH*) in 3–4 mice (2–4 sections per mouse) for each neuronal marker. *Confocal images of the NAc were taken from regions around the anterior commissure from coronal sections between Bregma 1.54 and 0.98 mm (*Paxinos and Franklin, 2012*).* The proportion of GPR83 positive cells that co-localized with either DARPP-32, ChAT or TH were calculated for each field. *Since GPR83/*

eGFP mice, and not GPR83 antibodies, were used to identify GPR83 expression, analysis of cell-type expression of GPR83 identifies transcript co-localization and not protein expression of GPR83. Data are represented as the percentage of cells that are positive for GPR83 transcript.

2.3 RNAscope In Situ Hybridization Assay

RNA in situ hybridization (ISH) was performed for GPR83 and eGFP on brain sections from GPR83/eGFP mice (Advanced Cell Diagnostics, Newark, CA). Brains were rapidly removed, frozen in isopentane (kept on dry ice) for 15 s, and then placed in a sealed bag for storage at − 80 °C. After equilibrating the tissue in a cryostat (Leica CM 3050S, *Buffalo Grove, Il*) at − 20 °C for 1 h, *brains were embedded in OCT media* and 20-μm brain slices of the NAc were collected and mounted directly onto Super Frost Plus slides (Fisher Scientific, *Waltham, MA*, Cat. no. 12-550-15). The slides were left at − 20 °C for 1 h and then stored at − 80 °C. Brain slices were fixed in 4% paraformaldehyde in 1x PBS for 1 h at 4°C. The slices were dehydrated in 50, 70 and 100% ethanol and stored in fresh 100% ethanol overnight at −20°C. Next day, the slides were first dried at room temperature for 5 min and a hydrophobic barrier was drawn on slides around brain slices. The slides were then treated with protease solution (Advanced Cell Diagnostics, Newark, CA) at room temperature for 30 min, followed by washing in 1x PBS. Subsequently, 1x target probes for GPR83 and eGFP were applied and the slides were incubated at 40°C for 2 h in the HybEZ oven. Slides were first incubated with preamplifier and amplifier probes (AMP1, 40°C for 30 min; AMP2, 40°C for 15 min; AMP3, 40°C for 30 min) and then with fluorescently labeled probes by selecting a specific combination of colors associated with each channel: green (Alexa 488 nm) and orange (Atto 550 nm) using AMP4 AltB. Sections were incubated for 30 s with DAPI. The slides were washed with 1x washing buffer two times between incubations. After air drying, the slides were cover slipped with a fluorescent mounting medium (Vector Labs, Burlingame, CA).

2.4 Morphine CPP

Morphine CPP was performed as described previously (Fakira et al., 2016; Portugal et al., 2014). Apparatus: Morphine conditioning occurred in a 3-chamber CPP apparatus from Med-Associates (*St. Albans, VT*). The neutral center chamber is 7.24 cm long, with smooth gray PVC plastic walls and floor, whereas the two conditioning chambers are 16.7 cm long, one with black walls and one with white walls. The floors are a metal grid pattern. The chambers are separated by automatic guillotine doors to allow access to all three chambers and photobeam arrays in all three chambers are controlled by Med-PC software (Med-associates, St. Albans, VT).

Morphine CPP design: See Fig 6A and 7E for schematic. On pre-conditioning day (day 1), male and female mice were placed in the neutral chamber and preference for all 3 chambers was measured for 15 min. Mice were randomly assigned to one of the two chambers. During training (days 2−5) mice received s.c. saline and were placed in the saline-paired chambers in the morning for 30 min. During the afternoon (4h later), mice received morphine (5, 10 or 20 mg/kg) s.c. and were placed in the morphine-paired compartment for 30 min. Control animals were treated with saline s.c. in both conditioning chambers. Place preference was

tested on day 6 by placing mice in the central compartment and allowing them 15 minutes to freely explore the apparatus. All experiments were counterbalanced between the white and black chamber pairings. Preference was measured by subtracting the amount of time spent in the morphine-paired chamber on preference testing day from the amount of time spent in that chamber on pre-conditioning day.

2.5 Morphine Home Cage Treatment

Experiments were performed as described previously (Fakira et al., 2016). Each day for four consecutive days, mice were injected with saline and returned to their home cage in the morning; four hours later mice were injected with saline or morphine (10 mg/kg) and returned to their home cage. On the fifth day, micropunches of the NAc were collected for qPCR analysis.

2.6 Quantitative PCR

Total cellular RNA was extracted using Qiazol reagent and the RNAeasy Midi kit (QIAGEN, Valencia, CA) from NAc punches of GPR83 wild type (WT) and KO mice. Total RNA was reverse transcribed into cDNA using VILO master mix (Invitrogen, Carlsbad, CA). qPCR was performed in triplicate aliquots from each individual animal with Power SYBR Green PCR master mix (ThermoFisher, *Waltham, MA*), 25 ng of cDNA and 0.5 μM of primers using an ABI Prism 7900HT (*Thermo Fisher, Waltham, MA*) in the qPCR CoRE at Icahn School of Medicine at Mount Sinai. Primer sequences are listed in Supplemental Table 1. The CT values for the technical replicates were averaged and analysis performed using the $\Delta\Delta C_T$ method and normalized to saline controls. In some cases, qPCR reactions were repeated to determine the reliability of the primers and RNA samples.

2.7 GPR83 shRNA and surgeries

Three weeks prior to behavioral testing, a craniotomy was performed under isoflurane anesthesia and 0.5 μL of lentiviral GPR83 shRNA or control shRNA particles (10^9; Sigma Mission Lentiviral Transduction Particles, *St. Louis, MO*) were infused into the NAc (A/P: +1.5, Lat: +/− 1.6, D/V:−4.4). The GPR83 shRNA targeted the sequence 5'-CCATGAGCAGTACTTGTTATA-3', an exonic region of the gene. A nucleotide BLAST of this sequence produces three alignments with E values of 0.003 that correspond to GPR83 variants; other alignments have E values greater than 40, indicating that this sequence has few off targets.

2.8 Fast Scanning Cyclic Voltammetry

300 μm-thick coronal brain sections containing the NAc were immersed in oxygenated aCSF containing (in mM): NaCl (126), KCl (2.5), NaH2PO4 (1.2), CaCl2 (2.4), MgCl2 (1.2), NaHCO3 (25), glucose (11), L-ascorbic acid (0.4) and pH was adjusted to 7.4. Sections were transferred to testing chambers containing aCSF at 32 °C with a 1 ml min−1 flow rate. A carbon fiber microelectrode (100–200 μM length, 7 μM radius) and a bipolar stimulating electrode were placed into the NAc. Dopamine release was evoked by a single electrical pulse (300 μA, 4 ms, monophasic) applied to the tissue every 5 min. Extracellular dopamine levels were recorded by applying a triangular waveform (−0.4 to +1.2, to −0.4 V versus Ag/

AgCl, 400 μV s−1). Once the peak of evoked dopamine release stabilized (three collections with <10% variability), the amount of evoked dopamine release and a maximal rate of uptake (Vmax) as well as decay rates (tau) were assessed. Subsequently, tonic and phasic stimulations were applied to slices. Tonic stimulations consisted of one pulse stimulations. Phasic stimulations consisted of five pulses at 5, 10 or 20 Hertz. These stimulation parameters were selected based on the physiological firing properties of ventral tegmental area (VTA) dopamine neurons *in vivo*. To determine the contribution of cholinergic signaling to dopamine release, tonic and phasic stimulations were done in the absence and presence of mecamylamine, a non-selective, non-competitive antagonist of nicotinic acetylcholine receptors.

To permit the corroboration between electrical current and dopamine concentration, recording electrodes were calibrated (in electrical current; nA) to a known concentration of dopamine (3 μM) using a flow-injection system. Demon voltammetry and analysis software (*Wake Forest Innovations, Winston-Salem, NC*) was used for all analysis of FSCV data (Yorgason et al., 2011). Data were modelled using both peak and decay curves and Michaelis–Menten kinetics to determine dopamine release uptake and decay measures.

2.10 Data Analysis

Significance level ($p<0.05$) and data are presented as mean ± SEM. Student's t-test, One-way ANOVA with Tukey's Multiple Comparisons test or two-way ANOVA with Bonferroni post-hoc tests were used when appropriate using GraphPad Prism (*San Diego, CA*).

3.0 Results

3.1 Cell-type expression of GPR83 in the reward pathway.

In situ hybridization (ISH) mRNA analysis of GPR83 in the Allen Brain Developing Mouse Atlas confirms high levels of GPR83 expression previously reported in the NAc (Fig 1A and B;(Brezillon et al., 2001; Lueptow et al., 2018; Müller et al., 2013; Pesini et al., 1998; Sah et al., 2007)). *Moreover, this analysis identifies an intense band of expression in the olfactory tubercle and piriform cortex and sparse staining throughout the cortex* (Fig 1A). To further examine GPR83 expression, we used GPR83/eGFP mice that label GPR83 positive cells with eGFP. Consistent with published studies, GPR83 is highly expressed in the NAc (Fig 1C and D). Higher magnification reveals eGFP expression in cells with neuronal morphology (Fig 1E). We further validated this expression using the RNAscope ISH assay. Probes for eGFP (green, Fig 1 F) and GPR83 (red, Fig 1G) are co-localized in individual cells (Fig 1H).

Striatal neurons are anatomically distinguished by the expression of distinct makers, including DARPP-32 for medium spiny neurons (MSNs) and ChAT for cholinergic interneurons (CIN) (Matamales et al., 2009; Ouimet and Greengard, 1990; Tepper et al., 2010). To investigate whether GPR83 expressing neurons are MSNs, immunofluorescence for GPR83 (GFP labeled) and DARPP-32 was performed in GPR83/eGFP mice. eGFP staining in GPR83/eGFP mice identified cells with neuronal morphology (Fig 2A and G). There was robust DARPP-32 staining (Fig 2B and H) in line with the fact that MSNs

comprise 95% of neurons in *the striatum* (Yager et al., 2015). The majority of GPR83 expressing neurons did not co-localize with DARPP-32 (Fig 2C and I) indicating that a large number of GPR83 expressing neurons in the striatum are not MSNs. Complementary studies using dynorphin as a marker for D1-type MSNs also indicate minimal GPR83 expression in MSNs (Supplemental Fig 2). However, the pattern of GPR83 expression suggests that GPR83 may be expressed in CINs. To investigate this, co-expression of GPR83 and ChAT was evaluated. GPR83 (Fig 2D and J) and ChAT (Fig 2E and K) expression overlap in a large portion of GPR83 expressing cells (Fig 2F and L). Quantification of co-expression of GPR83 and these markers indicate that ~80% of GPR83 positive cells are cholinergic and ~ 15% are DARPP-32 positive (Fig 2M). These data demonstrate that the majority of GPR83 expressing neurons are CINs.

There are both cholinergic interneurons, which only make synaptic contact with local neurons, and cholinergic projection neurons, whose axons project to other brain regions. Since GPR83 expression highly overlaps with CINs in the NAc, we evaluated whether GPR83 is expressed in cholinergic projection neurons as well. For these studies, brain sections that included the diagonal band nucleus (DBN), olfactory tubercle and the NAc were examined. Co-expression of GPR83 (Fig 2N) and ChAT (Fig 2O) only occurs in the NAc and olfactory tubercle (Fig 2P), as indicated by cells labeled with a star. Cholinergic projection neurons in the DBN do not express GPR83 (Fig 2 N–P). These data suggest that GPR83 is only expressed in CINs and not in cholinergic projection neurons found in the DBN.

Dopamine neurons project from the VTA to the NAc releasing dopamine onto MSNs in response to rewarding stimuli. ISH mRNA analysis of GPR83 by the Allen Brain Developing Mouse Atlas suggests that there are minimal levels of GPR83 expression in the VTA (Fig 3 A and B). Higher magnification of GPR83 ISH staining in the VTA (Fig 3 B1) compared to the mammillary bodies of the hypothalamus (Fig 3 B2(inset)) indicates that the VTA has moderate levels of GPR83. Tyrosine hydroxylase (TH) immunostaining in GPR83/eGFP mice was used to identify VTA dopamine neurons (Figure 3 C). Examination of VTA dopamine neurons indicate that they have a moderate level of GPR83 expression (Fig 3D; 3–3a–c) in comparison to mammillary neurons (Fig 3D; 3–4a–c). *Quantification of the co-localization between GPR83 and TH indicates that ~ 80% of GPR83 expressing neurons are dopamine neurons, and that 20% TH positive neurons do not express GPR83 (*Fig 3E*).* The expression pattern of GPR83 in CIN in the NAc and in VTA DA neurons suggests that GPR83 may regulate dopamine levels either by modulation of dopamine terminals locally in the NAc and/or by modulating dopamine neurons.

3.2 Analysis of dopamine release in GPR83 KO mice.

To examine the role of GPR83 in dopamine release in the NAc, FSCV was performed in slices from GPR83 WT and KO mice. Baseline dopamine release is enhanced *in NAc slices from GPR83 KO mice* compared to WT (Fig 4 A and B), which is independent of sex (Supplemental Fig 3). There were no significant changes in maximal dopamine uptake (Vmax) or dopamine uptake rate (tau; Fig 4C–E). Under normal conditions, tonic firing of VTA dopamine neurons releases low levels of dopamine; however, upon presentation of

rewarding stimuli, VTA dopamine neurons exhibit burst firing that leads to release of large amounts of dopamine and other mediators into the NAc (Chaudhury et al., 2013; Walsh et al., 2014). To examine whether GPR83 regulates dopamine release during burst firing, we measured dopamine release during phasic stimulation and found that it is significantly elevated in NAc slices from GPR83 KO mice versus WT (Fig 4F and G). However, when phasic dopamine release is normalized to baseline (tonic) dopamine release, it is revealed that the percent change in dopamine is blunted in slices from GPR83 KO mice compared to WT (Fig 4H and I). This data suggests that in GPR83 KO there is saturation of dopamine release, thereby blunting the ratio of phasic versus baseline dopamine.

Our studies show that GPR83 is expressed in CINs in the NAc, therefore GPR83 may be modulating their activity and thus release of acetylcholine. It is known that acetylcholine release from CIN enhances dopamine release via activation of nicotinic acetyl choline (nACh) receptors on dopamine terminals (Cachope et al., 2012; Threlfell et al., 2012). To investigate if this mechanism plays a role in the increased dopamine release in NAc slices from GPR83 KO mice, the nACh receptor antagonist mecamylamine (MEC; 2μM) was bath applied to slices from GRP83 KO and WT mice during tonic or phasic stimulation. Dopamine release, measured before and after the application of MEC, indicated an overall main effect of MEC on dopamine release in slices from both GPR83 WT and KO mice (Fig 4 J). However, post-hoc analysis revealed a significant inhibition of dopamine responses by MEC only at 1 pulse and 5 Hz stimulations compared to dopamine release pre-MEC in slices from GPR83 KO mice (Fig 4J). Overall, these data suggest that dopamine release in the NAc may be more sensitive to MEC in GPR83 KO mice compared to WT.

Since changes in dopamine synthesis may contribute to the enhanced dopamine release observed in GPR83 KO mice, we examined phosphorylation of TH (the rate limiting enzyme in dopamine synthesis) at serine 40 using western blots of the VTA. We found a decrease in TH phosphorylation in GPR83 KO mice compared to WT with no change in overall TH expression (Fig 5 A and B). There were no differences in actin levels between GPR83 WT or KO mice (Supplemental Figure 4). These data suggest that an increase in production of dopamine via TH activity is not responsible for the increase in dopamine release.

Since dopamine release in the NAc is enhanced in slices from GPR83 KO mice, we examined the expression of several dopamine related genes, including dopamine receptor type 1 and 2 (DRD1 and DRD2), catechol-O-methyltransferase (COMT), and kappa opiate receptors (OPRK) in the NAc of GPR83 KO mice. There were no changes in the gene expression for dopamine receptors DRD1 and DRD2 in male and female GPR83 KO mice (Fig 5C). COMT, an enzyme responsible for dopamine metabolism, is significantly increased in male but not in female GPR83 KO mice compared to WT (Fig 5C). Finally, in female GPR83 KO mice, there is a significant increase in OPRK expression that was not observed in the males (Figure 5C). Kappa opiate receptors play an important role in the motivational properties of drugs of abuse by regulating presynaptic dopamine in the NAc (Spanagel et al., 1992). These data suggest that COMT and OPRK gene expression are regulated by GPR83 in a sex-dependent manner supporting the notion that GPR83 is a potential regulator of the dopaminergic system.

3.3 Analysis of GPR83's role in morphine reward-learning.

We examined the effect of morphine reward on GPR83 and proSAAS expression in the NAc using morphine CPP (schematic Fig. 6A). We find that while both male and female mice spend more time in the morphine paired chamber compared to the saline paired chamber, female mice had significantly lower preference scores compared to the male mice (Fig 6B; average females: 84±10 vs males:171±24). These results demonstrate sex differences in morphine reward-learning. Next, we sought to determine whether there wasa relationship between morphine preference levels and GPR83 expression in the NAc. For these experiments, qPCR analysis for GPR83 in NAc punches was performed in a group of male and female mice trained in morphine CPP. We found a significant positive relationship between morphine preference scores and GPR83 expression such that higher levels of GPR83 expression were found in mice with larger preference scores (Fig 6C). Since female mice tend to have lower morphine preference scores compared to male mice, we compared GPR83 expression in the NAc of a select group of male and female mice which displayed similar levels of preference (Fig 6D and E insets; average males 116±17.5 s vs average females 106.2±43.69 s) to determine whether sex differences play a role in this relationship between morphine preference and GPR83 expression in the NAc. We also sought to determine whether morphine reward-learning regulates the expression of proSAAS, the precursor to the neuropeptide PEN. In both males and females, GPR83 expression was upregulated following morphine CPP with no change in proSAAS (Fig 6D and E) indicating that the strength of morphine preference and not sex is responsible for the relationship between morphine preference and GPR83 expression in the NAc and this is specific to GPR83 since proSAAS expression was not affected

Previous studies demonstrated that morphine-context learning differentially induces neuroadaptations compared to administration of morphine in the absence of novel cues (Fakira et al., 2016, 2014). To differentiate between expression changes induced by morphine-context learning versus morphine administration alone, mice were also treated with the same schedule and dose of morphine and immediately returned to their home cage (Fig 6F). Morphine treatment in the absence of novel contextual cues resulted in no change in GPR83 or proSAAS expression in either sex (Fig 6G and H). Together these results show that GPR83 expression is upregulated in mice given morphine-contextual associations but not by morphine alone.

Since dopamine release is enhanced in NAc slices from GPR83 KO mice, and morphine CPP regulates GPR83 expression in the NAc, we examined if GPR83 KO mice have any alterations in morphine CPP. There were no differences in morphine CPP between GPR83 WT and KO mice of either sex (Fig 7A). Since a global KO will have long–term effects on many circuits that influence drug reward, we also included GPR83 heterozygous (HT) mice. Morphine CPP was significantly attenuated in male GPR83 HT mice compared to WT and KO but not in female mice (Fig 7A). To determine whether the lack of effect in GPR83 KO mice may be due to a ceiling effect of morphine CPP at the 10 mg/kg dose, another set of GPR83 WT and KO mice underwent morphine CPP at a 5 mg/kg dose. There were no significant differences in morphine preference between WT and KO mice at 5 mg/kg dose of morphine (Fig 7B).

The attenuation of morphine CPP in GPR83 HT mice, and lack of effect in GPR83 KO indicates that global deletion of GPR83 may induce compensatory effects within circuits that regulate reward-learning or within the CIN interneurons in the NAc. To identify whether GPR83 expression within the NAc controls morphine reward-learning, we knocked down expression of the receptor using GPR83 or control shRNA lentiviral particles injected into the NAc of C57BL/6J mice (Fig 7C); this leads to a ~50% knockdown of GPR83 21 days post-injection (Fig 7D). Control or GPR83 shRNA lentivirus treated mice were subjected to morphine CPP using a 10 mg/kg dose over 4 days (Fig 7E). We find that GPR83 knockdown leads to a significant attenuation of morphine CPP in male but not in female mice (Fig 7F). However, female mice had significantly lower morphine preference than males. To determine whether the lack of effect of GPR83 knockdown in female mice is due to the dose of morphine administered (10 mg/kg dose), a second group of female mice treated with control or GPR83 shRNA lentivirus were subjected to morphine CPP using a higher dose of morphine (20 mg/kg; Fig 7E). In this case we find that female mice administered GPR83 shRNA lentivirus display a significantly attenuated morphine preference compared to mice given control lentivirus (Fig 7G). These data suggest that GPR83 expression in the NAc plays an active role in morphine reward-learning and that female mice have similar morphine preference compared to male mice when treated with a higher dose of morphine.

4.0 Discussion

Characterizing novel targets that regulate drug reward-learning may identify new and more effective therapeutics for substance abuse disorders. GPR83, an orphan receptor activated by the neuropeptide PEN, is highly expressed in the NAc, an important brain region in the mesolimbic reward pathway; however, the role of GPR83 in this pathway is understudied. We therefore sought to characterize GPR83 in the reward pathway by examining the cell types expressing the receptor, and by examining the impact of GPR83 on dopamine signaling and in reward-learning using a morphine CPP model. Our studies show that GPR83 is predominately expressed in CINs in the NAc with moderate expression in dopamine neurons in the VTA. Enhanced baseline dopamine release was observed in NAc slices from GPR83 KO mice, therefore blunting the ratio of phasic versus tonic dopamine. We show altered expression of several dopamine related genes/proteins, and that dopamine responses are more sensitive to the nAChR antagonist, MEC, in GPR83 KO mice, supporting the notion that GPR83 expression in CINs may be in part responsible for enhanced dopamine release. Furthermore, GPR83 expression in the NAc is upregulated in response to morphine-reward learning, but not when morphine is administered in the home cage, and GPR83 knockdown in the NAc attenuates morphine reward. Finally, these studies uncovered *sex differences in the rewarding effects of morphine, where female mice required a higher dose to achieve similar preference levels as male mice*.

Original reports of GPR83 showed that this receptor is expressed in the brain and thymus (Harrigan et al., 1989). Subsequent studies evaluated the pattern of GPR83 expression across brain regions at the mRNA level using ISH in rat, mouse and human, demonstrating strong to moderate GPR83 expression in the NAc, dorsal striatum, amygdala, hypothalamus, hippocampus and cortical regions (Brezillon et al., 2001; Lueptow et al., 2018; Pesini et al., 1998; Sah et al., 2005). Our current studies using GPR83/eGFP mice confirm these findings,

identifying GPR83 expression throughout the NAc and dorsal striatum. Additionally, we have identified moderate expression of GPR83 in VTA dopamine neurons. Although this was unexpected based on the GPR83 ISH analysis in the Allen Brain Developing Mouse brain, it is supported by studies showing GPR83 expression in dopamine neurons using several methods including single-cell RNAseq analysis, laser capture microdissection and microarray analysis (Chung et al., 2005; Kramer et al., 2018; Viereckel et al., 2016). Therefore, it appears that ISH analysis may not be sensitive enough to detect the GPR83 expression in this brain region. In fact, ISH analysis by (Viereckel et al., 2016) was also unable to detect GPR83 in the VTA while our studies uncovered GPR83 expression in VTA dopamine neurons using GPR83/eGFP reporter mice.

Our studies show that morphine CPP upregulates GPR83 expression in the NAc in both male and female mice. GPR83 was originally described as a glucocorticoid induced receptor (Adams et al., 2003; Maureen T Harrigan et al., 1991). Previous studies have demonstrated that acute administration of morphine increases the levels of the glucocorticoid, corticosterone (Esmaeili-Mahani et al., 2008; Kiem et al., 1991; Yamamoto et al., 2011); therefore, this increase in GPR83 expression may be due to a direct effect of morphine or morphine-induced release of glucocorticoids. Previous studies identified that amphetamine also increases GPR83 expression in the medial prefrontal cortex (Wang et al., 2001); however, amphetamine also induces a release of corticosterone (Stairs et al., 2011). Therefore, it still remains unclear whether the drug-mediated increase in GPR83 is due to a drug-induced release of corticosterone.

Morphine reward-learning was affected by local GPR83 knockdown in the NAc and not in GPR83 KO mice. Since GPR83 KO removes the receptor from the entire brain, there may be effects in other circuits that interact with the reward pathway making this result difficult to interpret. In fact, we found that morphine CPP was attenuated in male GPR83 heterozygous mice, a model in which GPR83 expression is decreased but not totally removed. The result is similar to our observations when GPR83 was locally knocked down indicating that global KO may be affecting other brain regions or altering other signaling pathways. In fact, we observed alterations in the expression of several dopamine related proteins suggesting that chronic deletion of GPR83 may result in systemic regulation of proteins. The lack of effect in morphine CPP in the GPR83 KO appears to be in contrast to our finding that dopamine release is enhanced in GPR83 KO mice. One possible explanation for this is that in the FSCV studies, where we uncovered enhanced dopamine release in the NAc, dopamine release was induced by directly stimulating terminals in the NAc, thereby minimizing influence from other circuits.

There is some evidence that the endogenous ligand PEN is also involved in drug-reward processing. Studies found proSAAS peptides, including PEN, to be decreased in the VTA and NAc following cocaine administration (Berezniuk et al., 2017). Our studies did not find any differences in proSAAS mRNA expression following morphine CPP in the NAc. There are several reasons for the differences between these studies. First, our studies focused on morphine, which is an opioid, while the proSAAS studies examined the stimulant cocaine. Also, the proSAAS study examined the presence of the peptides directly, while our studies examined the expression of the proSAAS transcript. In terms of behavioral effects, proSAAS

KOs had blunted locomotor sensitization to both amphetamine and cocaine; however, there were no differences in cocaine CPP at several doses tested (Berezniuk et al., 2017). In our studies, there was no effect of GPR83 KO on morphine CPP which is similar to the proSAAS KO studies; however, we did observe an effect with local knockdown indicating that global KOs may not be the ideal model for these studies. Further investigation is needed to confirm whether PEN-mediated activation of GPR83 regulates reward-learning.

Our data suggests that GPR83 expression is regulated by the formation of drug-context associations. CIN activity in the striatum is responsible for processing contextual cues related to reward processing (Aosaki et al., 1995, 1994; Apicella, 2007; Apicella et al., 1991; Kimura et al., 2006). This concept has been confirmed for CINs in the NAc by the studies showing that their stimulation blunts and their inhibition augments cue-motivated behavior (Collins et al., 2019). In fact, CIN activity regulates glutamatergic plasticity that underlies extinction cocaine-context associations in the NAc (Lee et al., 2016). The current studies demonstrate that GPR83 expression is localized to CINs and that GPR83 knockdown in the NAc blunts morphine CPP, a paradigm that is highly dependent on the formation of drug-context associations. Therefore, decreasing GPR83 expression or activity may regulate CIN function, and thus the motivation for drug seeking induced by contextual cues. These data suggest that GPR83 may be a target for the treatment of substance abuse; however, more studies are needed to further characterize this receptor, including studies investigating the effect of GPR83 on drug self-administration.

Another function of CINs is the regulation of dopamine release via activation of nAChRs on dopamine terminals in the NAc (Cachope et al., 2012; Threlfell et al., 2012; Zhou et al., 2001). Here, we found that GPR83 is localized on CINs, dopamine release is enhanced in GPR83 KO NAc, and that the regulation of dopamine release by nACh receptors is more sensitive in GPR83 KO mice. Together, these findings further suggest that GPR83 is a regulator of CIN activity. Analysis of proteins involved in the regulation of dopamine in the NAc of GPR83 KO mice revealed a down regulation of TH phosphorylation and an upregulation of genes responsible for clearing dopamine or blocking dopamine release. This may suggest that in GPR83 KO mice, there is a chronic increase in dopamine which then leads to regulation of dopamine related proteins as a mechanism to overcome the elevated dopamine levels. Tools to acutely activate or inhibit GPR83 are needed to determine whether our results reflect adaptive changes resulting from chronic downregulation or deletion of GPR83, or whether acute inhibition of GPR83 can modulate CIN activity and dopamine release effecting morphine-reward learning.

We observed sex-differences in morphine reward such that females required twice the dose of morphine to develop a similar level of preference as males. Sex-differences have been observed in morphine-induced antinociception, self-administration, CPP and withdrawal symptoms(Alexander et al., 1978; Cicero et al., 1997, 2003, 2002, 2000, 1996; Hadaway et al., 1979). However, to our knowledge there is no study demonstrating sex-differences observed in the current studies. Previous studies in rats demonstrated that females had a stronger preference for morphine at similar doses as used in this study (Cicero et al., 2000). In terms of morphine's antinociceptive effects, Cicero et al.,(1997, 1996) demonstrated that female rats are less sensitive to morphine. Additionally, female rats self-administer larger

amounts of opioids (Alexander et al., 1978; Cicero et al., 2003; Hadaway et al., 1979) and have lower levels of physical withdrawal symptoms (Cicero et al., 2002) compared to males. While the differences in morphine preference in our studies versus others is apparent, our finding that higher doses of morphine are required for female mice to develop similar preference levels compared to males fits well with the concept that females are less sensitive to morphine antinociception, administer greater amounts of opioids and feel less withdrawal symptoms. There are several explanations for these differences observed in morphine reward, including stress and estrus cycle dependent effects. For example, when rats are exposed to a stressor, males have a higher morphine preference than females (Abad et al., 2016), similar to our observations. Evidence suggests that corticosterone regulates morphine antinociception and consumption (Alexander et al., 1978; Esmaeili-Mahani et al., 2008; Hadaway et al., 1979). In support of this, female mice have higher baseline corticosterone levels (Vassoler et al., 2018) and adrenalectomized rats have increased sensitivity to morphine antinociception that is reversed by administration of corticosterone (Esmaeili-Mahani et al., 2008). Therefore, in our studies it is possible that corticosterone levels in female mice may be responsible for the differences in morphine preference observed between males and females. Another concept worth considering is that females respond to drug rewards differently depending on their stage in the estrus cycle (Calipari et al., 2017). In the current study, we did not investigate the impact of the estrus cycle on morphine preference, therefore future studies will be necessary to determine this relationship.

5.0 Conclusions

In summary, our studies found that GPR83 regulates morphine reward and dopamine release in the NAc. This receptor is expressed at high levels in CINs in the NAc and at moderate levels in VTA dopamine neurons. Based on the fact that increases in CIN activation produce increases in dopamine release, GPR83 may play a role in CIN excitability. Future studies are needed to thoroughly examine the functional impact of GPR83 activation by PEN in these neurons and the relationship between PEN-mediated activation of GPR83 and dopamine responses/reward behaviors.

Supplementary Material

Refer to Web version on PubMed Central for supplementary material.

Acknowledgements:

The authors wish to thank Andrei Jeltyi for assistance in genotyping and animal husbandry and Dr. Ivone Gomes and Seshat Mack for careful reading of the manuscript. This work was supported by NIH grants R01-DA008863 and R01-NS026880 (to LAD), DA042111 and funding from the Brain and Behavior Research Foundation (to ESC), R01-AA022445, R56-MH115409 and R21-MH112081 (to MHH). Authors have no conflict of interest.

Abbreviations:

CIN	cholinergic interneuron
NAc	nucleus accumbens
VTA	ventral tegmental area

CPP	conditioned place preference
FSCV	fast scanning cyclic voltammetry
MSN	medium spiny neuron
DARPP-32	dopamine- and cAMP-regulated phosphoprotein
nACh	nicotinic acetyl choline receptor
MEC	mecamylamin

References

Abad ATK, Miladi-Gorji H, Bigdeli I, 2016 Effects of swimming exercise on morphine-induced reward and behavioral sensitization in maternally-separated rat pups in the conditioned place preference procedure. Neurosci. Lett 10.1016/j.neulet.2016.08.011

Adams F, Grassie M, Shahid M, Hill DR, Henry B, 2003 Acute oral dexamethasone administration reduces levels of orphan GPCR glucocorticoid-induced receptor (GIR) mRNA in rodent brain: Potential role in HPA-axis function. Mol. Brain Res 117, 39–46. 10.1016/S0169-328X(03)00280-8 [PubMed: 14499479]

Alexander BK, Coambs RB, Hadaway PF, 1978 The effect of housing and gender on morphine self-administration in rats. Psychopharmacology (Berl) 10.1007/BF00426903

Aosaki T, Kimura M, Graybiel AM, 1995 Temporal and spatial characteristics of tonically active neurons of the primate's striatum. J. Neurophysiol 10.1152/jn.1995.73.3.1234

Aosaki T, Tsubokawa H, Ishida A, Watanabe K, Graybiel AM, Kimura M, 1994 Responses of tonically active neurons in the primate's striatum undergo systematic changes during behavioral sensorimotor conditioning. J. Neurosci

Apicella P, 2007 Leading tonically active neurons of the striatum from reward detection to context recognition. Trends Neurosci 10.1016/j.tins.2007.03.011

Apicella P, Scarnati E, Schultz W, 1991 Tonically discharging neurons of monkey striatum respond to preparatory and rewarding stimuli. Exp. Brain Res 10.1007/BF00230981

Berezniuk I, Rodriguiz RM, Zee ML, Marcus DJ, Pintar J, Morgan DJ, Wetsel WC, Fricker LD, 2017 ProSAAS-derived peptides are regulated by cocaine and are required for sensitization to the locomotor effects of cocaine. J. Neurochem 10.1111/jnc.14209

Brezillon S, Detheux M, Parmentier M, Hokfelt T, Hurd YL, 2001 Distribution of an orphan G-protein coupled receptor (JP05) mRNA in the human brain. Brain Res 921, 21–30. https://doi.org/S0006-8993(01)03068-2 [pii] [PubMed: 11720708]

Cachope R, Mateo Y, Mathur BN, Irving J, Wang HL, Morales M, Lovinger DM, Cheer JF, 2012 Selective activation of cholinergic interneurons enhances accumbal phasic dopamine release: Setting the tone for reward processing. Cell Rep 2, 33–41. 10.1016/j.celrep.2012.05.011 [PubMed: 22840394]

Calipari ES, Juarez B, Morel C, Walker DM, Cahill ME, Ribeiro E, Roman-Ortiz C, Ramakrishnan C, Deisseroth K, Han MH, Nestler EJ, 2017 Dopaminergic dynamics underlying sex-specific cocaine reward. Nat. Commun 10.1038/ncomms13877

Chaudhury D, Walsh JJ, Friedman AK, Juarez B, Ku SM, Koo JW, Ferguson D, Tsai HC, Pomeranz L, Christoffel DJ, Nectow AR, Ekstrand M, Domingos A, Mazei-Robison MS, Mouzon E, Lobo MK, Neve RL, Friedman JM, Russo SJ, Deisseroth K, Nestler EJ, Han MH, 2013Rapid regulation of depression-related behaviours by control of midbrain dopamine neurons. Nature 10.1038/nature11713

Chung CY, Seo H, Sonntag KC, Brooks A, Lin L, Isacson O, 2005 Cell type-specific gene expression of midbrain dopaminergic neurons reveals molecules involved in their vulnerability and protection. Hum. Mol. Genet 10.1093/hmg/ddi178

Cicero T, Nock B, Meyer E, 1997 Sex-related differences in morphine's antinociceptive activity: relationship to serum and brain morphine concentrations. J. Pharmacol. Exp. Ther

Cicero TJ, Aylward SC, Meyer ER, 2003 Gender differences in the intravenous self-administration of mu opiate agonists. Pharmacol. Biochem. Behav 10.1016/S0091-3057(02)01039-0

Cicero TJ, Ennis T, Ogden J, Meyer ER, 2000 Gender differences in the reinforcing properties of morphine. Pharmacol. Biochem. Behav 10.1016/S0091-3057(99)00174-4

Cicero TJ, Nock B, Meyer ER, 2002 Gender-linked differences in the expression of physical dependence in the rat. Pharmacol. Biochem. Behav 10.1016/S0091-3057(02)00740-2

Cicero TJ, Nock B, Meyer ER, 1996 Gender-related differences in the antinociceptive properties of morphine. J. Pharmacol. Exp. Ther

Collins AL, Aitken TJ, Huang I-W, Shieh C, Greenfield VY, Monbouquette HG, Ostlund SB, Wassum KM, 2019 Nucleus accumbens cholinergic interneurons oppose cue-motivated behavior. Biol. Psychiatry 10.1016/j.biopsych.2019.02.014

Esmaeili-Mahani S, Javan M, Motamedi F, Ahmadiani A, 2008 Post-adrenalectomy changes in the gene expression of specific G-protein subunits involved in morphine sensitization. Neuropeptides 10.1016/j.npep.2007.12.002

Fakira AK, Massaly N, Cohensedgh O, Berman A, Moron JA, 2016 Morphine-Associated Contextual Cues Induce Structural Plasticity in Hippocampal CA1 Pyramidal Neurons. Neuropsychopharmacology 10.1038/npp.2016.69

Fakira AK, Portugal GS, Carusillo B, Melyan Z, Morón JA, 2014 Increased small conductance calcium-activated potassium type 2 channel-mediated negative feedback on N-methyl-D-aspartate receptors impairs synaptic plasticity following context-dependent sensitization to morphine. Biol. Psychiatry 75, 105–114. 10.1016/j.biopsych.2013.04.026 [PubMed: 23735878]

Gomes I, Bobeck EN, Margolis EB, Gupta A, Sierra S, Fakira AK, Fujita W, Müller TD, Müller A, Tschöp MH, Kleinau G, Fricker LD, Devi LA, 2016 Identification of GPR83 as the receptor for the neuroendocrine peptide PEN. Sci. Signal 9 10.1126/scisignal.aad0694

Hadaway PF, Alexander BK, Coambs RB, Beyerstein B, 1979 The effect of housing and gender on preference for morphine-sucrose solutions in rats. Psychopharmacology (Berl) 10.1007/BF00431995

Harrigan MT, Baughman G, Campbell NF, Bourgeois S, 1989 Isolation and characterization of glucocorticoids- and cyclic AMP-induced genes in T lymphocytes. Mol. Cell. Biol 9, 3438–3446. [PubMed: 2552295]

Harrigan MT, Campbell NF, Bourgeois S, 1991 Identification of a gene induced by glucocorticoids in murine T-cells: a potential G protein-coupled receptor. Mol.Endocrinol 5, 1331–1338. 10.1210/mend-5-9-1331 [PubMed: 1663214]

Harrigan, Maureen T, Campbell NF, Bourgeois S, 1991 Identification of a gene induced by glucocortocoids in murine T-cells:A potential G protein-coupled receptor. Mol. Endocrinol 5, 1331–1338. [PubMed: 1663214]

Kiem DT, Bartha L, Makara GB, 1991 Effect of dexamethasone implanted in different brain areas on the morphine-induced PRL, GH and ACTH/corticosterone secretion. Brain Res 10.1016/0006-8993(91)91521-2

Kimura M, Rajkowski J, Evarts E, 2006 Tonically discharging putamen neurons exhibit set-dependent responses. Proc. Natl. Acad. Sci 10.1073/pnas.81.15.4998

Koob G, Kreek MJ, 2007 Stress, dysregulation of drug reward pathways, and the transition to drug dependence. Am. J. Psychiatry 10.1176/appi.ajp.2007.05030503

Koob GF, 2008 A Role for Brain Stress Systems in Addiction. Neuron 10.1016/j.neuron.2008.06.012

Kramer DJ, Risso D, Kosillo P, Ngai J, Bateup HS, 2018 Combinatorial Expression of Grp and Neurod6 Defines Dopamine Neuron Populations with Distinct Projection Patterns and Disease Vulnerability. Eneuro 10.1523/ENEURO.0152-18.2018

Lee J, Finkelstein J, Choi JYY, Witten IBB, 2016 Linking Cholinergic Interneurons, Synaptic Plasticity, and Behavior during the Extinction of a Cocaine-Context Association. Neuron 10.1016/j.neuron.2016.05.001

Lu LF, Gavin MA, Rasmussen JP, Rudensky AY, 2007 GPR83 is dispensable for the development and function of regulatory T cells. Mol Cell Biol

Lueptow LM, Devi LA, Fakira AK, 2018 Targeting the Recently Deorphanized Receptor GPR83 for the Treatment of Immunological, Neuroendocrine and Neuropsychiatric Disorders. Prog. Mol. Biol. Transl. Sci 10.1016/bs.pmbts.2018.07.002

Matamales M, Bertran-Gonzalez J, Salomon L, Degos B, Deniau JM, Valjent E, Hervé D, Girault JA, 2009 Striatal medium-sized spiny neurons: Identification by nuclear staining and study of neuronal subpopulations in BAC transgenic mice. PLoS One. 10.1371/journal.pone.0004770

Müller TD, Muller A, Yi CX, Habegger KM, Meyer CW, Gaylinn BD, Finan B, Heppner K, Trivedi C, Bielohuby M, Abplanalp W, Meyer F, Piechowski CL, Pratzka J, Stemmer K, Holland J, Hembree J, Bhardwaj N, Raver C, Ottaway N, Krishna R, Sah R, Sallee FR, Woods SC, Perez-Tilve D, Bidlingmaier M, Thorner MO, Krude H, Smiley D, DiMarchi R, Hofmann S, Pfluger PT, Kleinau G, Biebermann H, Tschöp MH, 2013 The orphan receptor Gpr83 regulates systemic energy metabolism via ghrelin-dependent and ghrelin-independent mechanisms. Nat. Commun 4 10.1038/ncomms2968

Ouimet CC, Greengard P, 1990 Distribution of DARPP-32 in the basal ganglia: an electron microscopic study. J. Neurocytol 10.1007/BF01188438

Paxinos G, Franklin KBJ, 2012 Paxinos and Franklin's the Mouse Brain in Stereotaxic Coordinates, São Paulo, Academic Press.

Pesini P, Detheux M, Parmentier M, Hökfelt T, 1998 Distribution of a glucocorticoid-induced orphan receptor (JP05) mRNA in the central nervous system of the mouse. Mol. Brain Res 57, 281–300. 10.1016/S0169-328X(98)00099-0 [PubMed: 9675427]

Portugal GS, Al-Hasani R, Fakira AK, Gonzalez-Romero JL, Melyan Z, McCall JG, Bruchas MR, Morón JA, 2014. Hippocampal long-term potentiation is disrupted during expression and extinction but is restored after reinstatement of morphine place preference. J. Neurosci 34 10.1523/JNEUROSCI.2838-13.2014

Sah R, Parker SL, Sheriff S, Eaton K, Balasubramaniam A, Sallee FR, 2007 Interaction of NPY compounds with the rat glucocorticoid-induced receptor (GIR) reveals similarity to the NPY-Y2 receptor. Peptides 28, 302–309. 10.1016/j.peptides.2006.11.013 [PubMed: 17240481]

Sah R, Pritchard LM, Richtand NM, Ahlbrand R, Eaton K, Sallee FR, Herman JP, 2005 Expression of the glucocorticoid-induced receptor mRNA in rat brain. Neuroscience 133, 281–92. 10.1016/j.neuroscience.2005.01.066 [PubMed: 15893650]

Spanagel R, Herz A, Shippenberg TS, 1992 Opposing tonically active endogenous opioid systems modulate the mesolimbic dopaminergic pathway. Proc. Natl. Acad. Sci. U. S. A 10.1073/pnas.89.6.2046

Stairs DJ, Prendergast MA, Bardo MT, 2011 Environmental-induced differences in corticosterone and glucocorticoid receptor blockade of amphetamine self-administration in rats. Psychopharmacology (Berl) 10.1007/s00213-011-2448-4

Tepper JM, Tecuapetla F, Koós T, Ibáñez-Sandoval O, 2010 Heterogeneity and Diversity of Striatal GABAergic Interneurons. Front. Neuroanat 10.3389/fnana.2010.00150

Threlfell S, Lalic T, Platt NJ, Jennings KA, Deisseroth K, Cragg SJ, 2012 Striatal dopamine release is triggered by synchronized activity in cholinergic interneurons. Neuron 75, 58–64. 10.1016/j.neuron.2012.04.038 [PubMed: 22794260]

Vassoler FM, Toorie AM, Byrnes EM, 2018 Transgenerational blunting of morphine-induced corticosterone secretion is associated with dysregulated gene expression in male offspring. Brain Res 10.1016/j.brainres.2017.11.004

Viereckel T, Dumas S, Smith-Anttila CJA, Vlcek B, Bimpisidis Z, Lagerström MC, Konradsson-Geuken A, Wallén-Mackenzie A, 2016 Midbrain Gene Screening Identifies a New Mesoaccumbal Glutamatergic Pathway and a Marker for Dopamine Cells Neuroprotected in Parkinson's Disease. Sci. Rep 10.1038/srep35203

Walsh JJ, Friedman AK, Sun H, Heller EA, Ku SM, Juarez B, Burnham VL, Mazei-Robison MS, Ferguson D, Golden SA, Koo JW, Chaudhury D, Christoffel DJ, Pomeranz L, Friedman JM, Russo SJ, Nestler EJ, Han MH, 2014 Stress and CRF gate neural activation of BDNF in the mesolimbic reward pathway. Nat. Neurosci 10.1038/nn.3591

Wang DZ, Herman JP, Pritchard LM, Spitzer RH, Ahlbrand RL, Kramer GL, Petty F, Sallee FR, Richtand NM, 2001 Cloning, expression, and regulation of a glucocorticoid-induced receptor in rat brain: Effect of repetitive amphetamine. J. Neurosci 21, 9027–9035. [PubMed: 11698613]

Yager LM, Garcia AF, Wunsch AM, Ferguson SM, 2015 The ins and outs of the striatum: Role in drug addiction. Neuroscience 10.1016/j.neuroscience.2015.06.033

Yamamoto A, Kiguchi N, Kobayashi Y, Maeda T, Ueno K, Yamamoto C, Kishioka S, 2011 Pharmacological relationship between nicotinic and opioid systems in analgesia and corticosterone elevation. Life Sci 10.1016/j.lfs.2011.10.004

Yorgason JT, España RA, Jones SR, 2011 Demon Voltammetry and Analysis software: Analysis of cocaine-induced alterations in dopamine signaling using multiple kinetic measures. J. Neurosci. Methods 10.1016/j.jneumeth.2011.03.001

Zhou FM, Liang Y, Dani JA, 2001 Endogenous nicotinic cholinergic activity regulates dopamine release in the striatum. Nat. Neurosci 10.1038/nn769

Highlights

1. GPR83 is expressed on cholinergic interneurons in the NAc and dopamine neurons in the VTA.
2. Dopamine release in NAc slices is enhanced in GPR83 KO mice.
3. Morphine-reward learning upregulates GPR83 expression in the NAc while GPR83 knockdown attenuates reward-learning.
4. There are sex differences in morphine reward-learning.

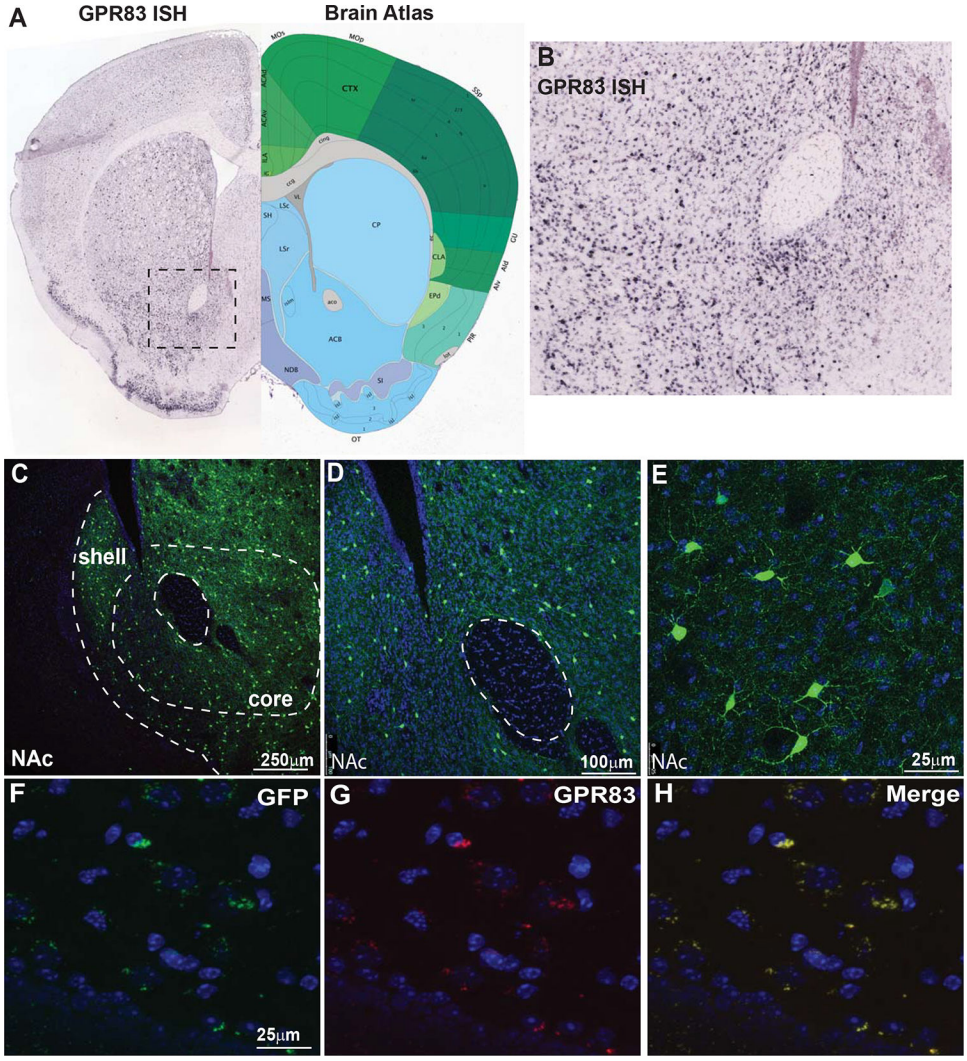

Figure 1: GPR83 expression in the NAc.

A) *In situ* hybridization (ISH) image from the Allen Brain Developing Mouse Atlas of GPR83 (Left) and corresponding brain atlas image (right) of a striatal brain section. **B)** Enlarged image of area within boxed image in **A)** demonstrating the pattern of GPR83 expression within the NAc. **C)** Low magnification image of GPR83 (green) expression in the NAc using GPR83 reporter mice from Gensat. **D)** and **E)** Higher magnification images showing that GPR83 is expressed in neurons in the NAc. RNAscope ISH probes for **F)** eGFP (green) and **G)** GPR83 (red) show that these markers colocalize **H)** in the same cells in GPR83/eGFP mice.

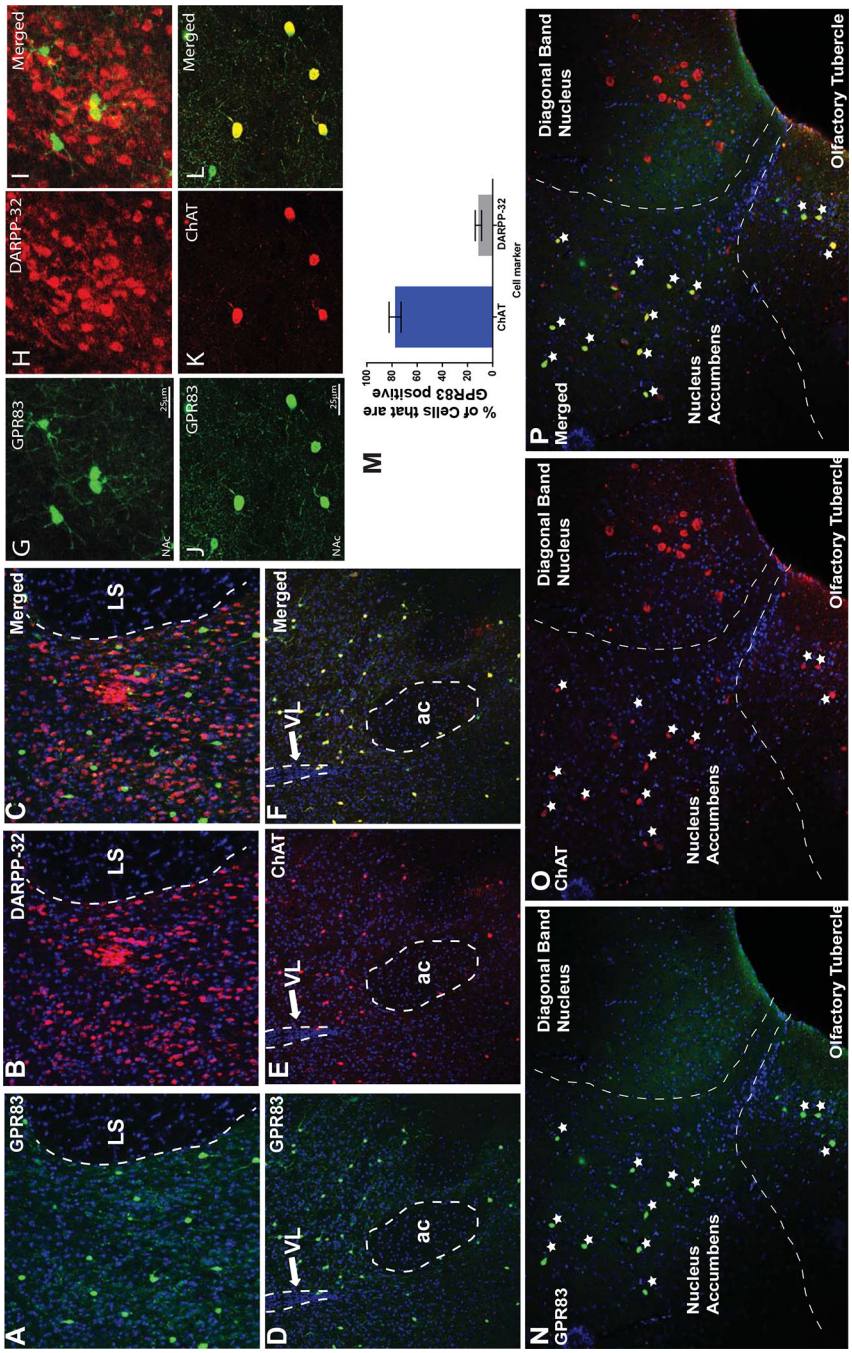

Figure 2: Cell-type expression of GPR83 in the NAc.

A) GPR83 (green) and **B)** DARPP-32 (red) expression in the NAc shows that GPR83 is not **C)** co-localized in medium spiny neurons. *Region to the right of the dashed lines is the lateral septum (LS).* **D)** GPR83 (green) and **E)** choline acetyltransferase (ChAT; red) expression in the NAc showing that GPR83 is **F)** co-localized in cholinergic interneurons (yellow). *The regions outlined by dashed lines are the anterior commissure (ac) and lateral ventricles (VL).* Higher magnification images of GPR83, DARPP-32 **(G-I)** and ChAT **(J-L)** expression. **M)** Quantification of percentage of GPR83 expressing cells that co-express

ChAT and DARPP-32. **N)** GPR83 (green) and **O)** ChAT (red) are only co-expressed **P)** in neurons in the NAc and olfactory tubercle, outlined by dashed lines. ChAT positive neurons in the Diagonal Band Nucleus do not express GPR83 **O)** and **P).** Co-expressing neurons are indicated by a star. The data represents mean ± SEM. Representative images of 15 sections from 4 mice for ChAT staining and 10 sections from 4 mice for DARPP-32 staining are shown.

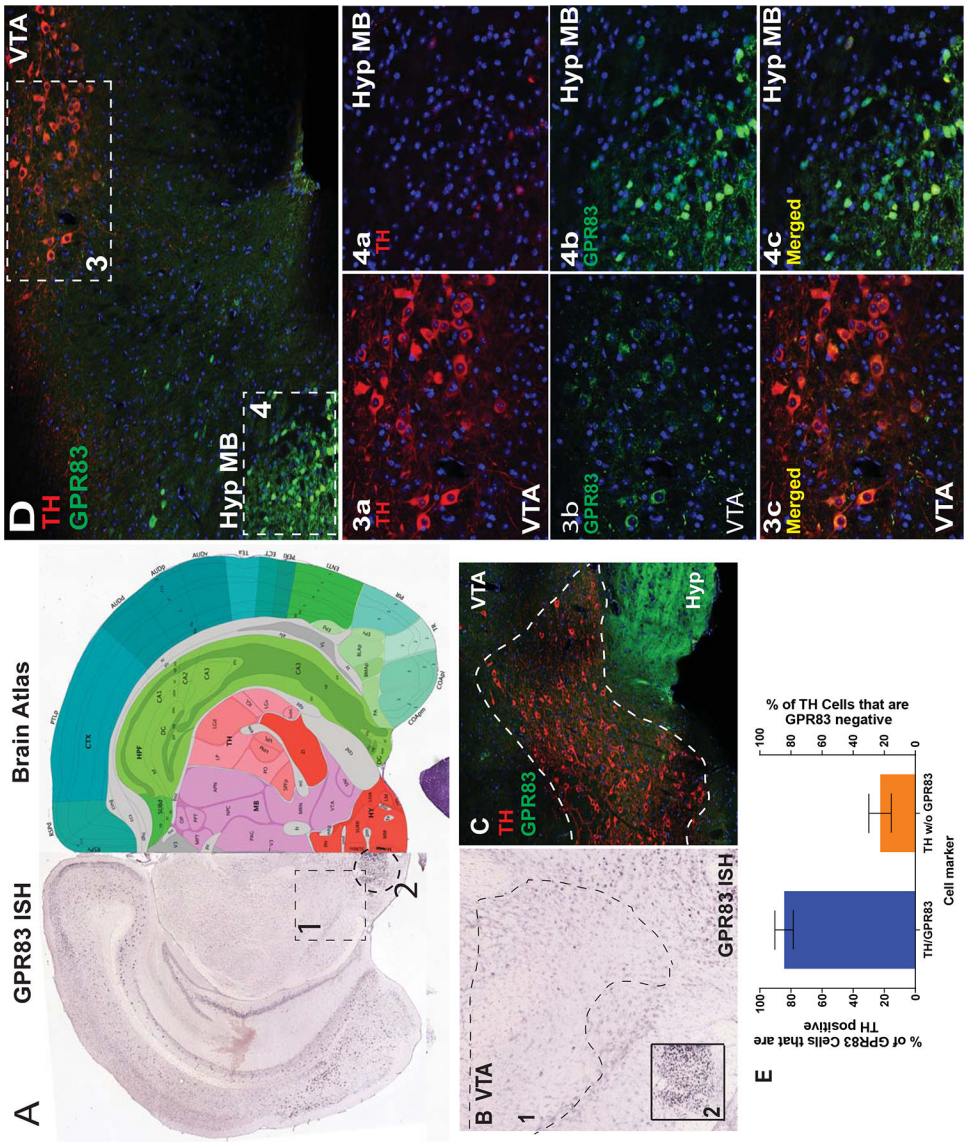

Figure 3: GPR83 expression within the VTA.

A) ISH image from the Allen Brain Developing Mouse Atlas of GPR83 (Left) and corresponding brain atlas image (right) of a brain section containing the VTA. **B1)** Enlarged 26 image of area within boxed outline in **A)** demonstrating the pattern of GPR83 expression within the VTA. **B2)** Enlarged image of area within the circled outline in **A)** demonstrating a brain region (hypothalamic mammillary bodies (MB)) which has high GPR83 expression compared to VTA. **C)** Brain section from GPR83/eGFP mice containing the VTA and mammillary bodies stained with TH and GFP. **D**) Brain section from GPR83/eGFP mice containing the VTA and mammillary bodies stained with TH and GFP. Boxed region **3)** contains VTA dopamine neurons and boxed region **4)** hypothalamic mammillary bodies. **3a)** Enlarged image of TH staining from boxed region (3) in **D)** and **3b)** is the same region with staining for eGFP (GPR83). **3c)** Merged image of 3a and 3b. **4a)** Enlarged image of TH staining from boxed (4) region in **D)** and **4b)** is the same region with staining for GFP (GPR83). **4c)** Merged image of 4a and 4b. Representative images of 8 sections from 2 mice

are shown. E) Quantification of percentage of GPR83 expressing cells that co-express TH and percentage of TH expressing cells that do not co-express GPR83. Representative images of 7 sections from 2 mice.

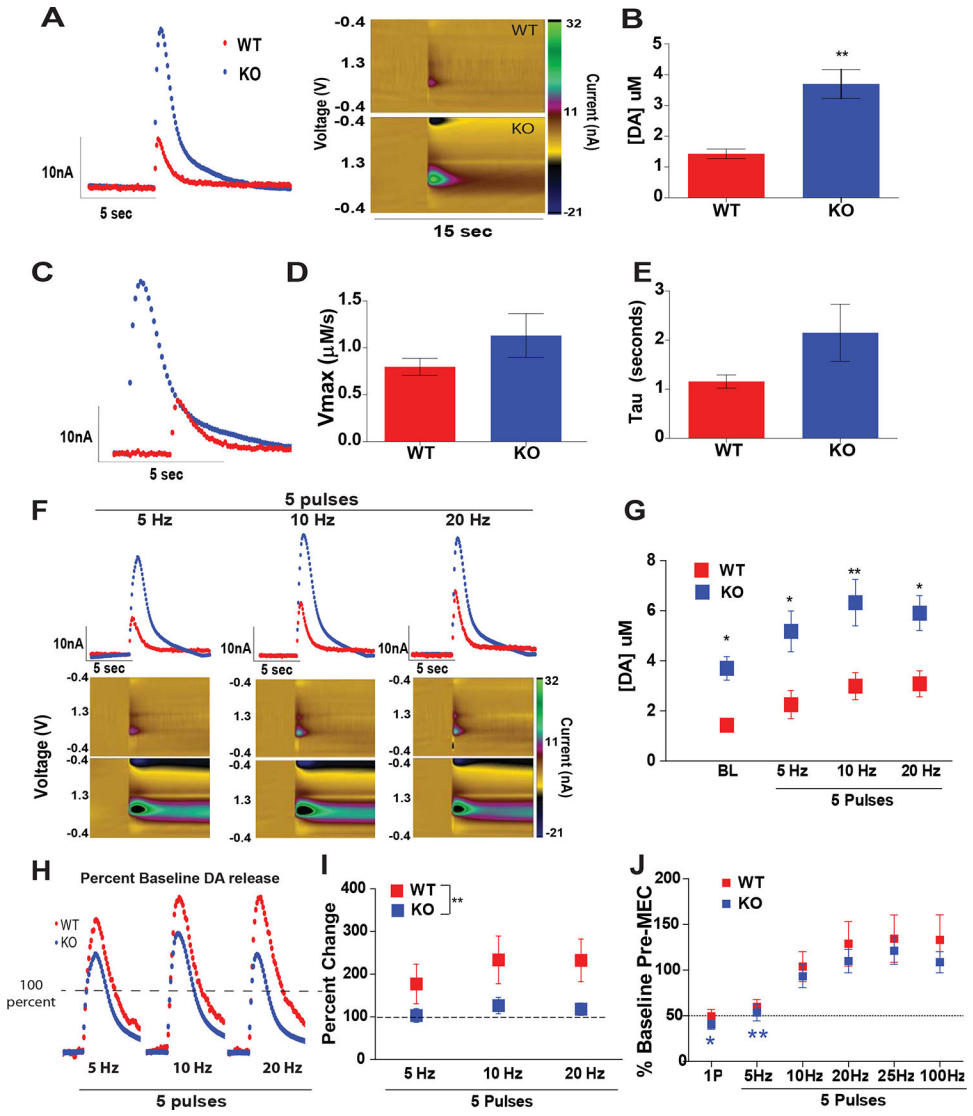

Figure 4: Analysis of dopamine responses in the NAc of GPR83 KO mice.

Fast scanning cyclic voltammetry in the NAc of GPR83 WT and KO mice was used to examine differences in dopamine release. **A)** Current versus time plots (left) and color plots (right) showing dopamine responses following single pulse stimulations. **B)** Grouped data from **A)** showing enhanced dopamine release in GPR83 KO mice compared to WT (Unpaired t-test; $t_{(8)}$=3.794, p<0.01, n=4–6). **C)** Aligned current versus time plots for measurement of dopamine uptake. Grouped data for **D)** maximal dopamine uptake (Vmax, Unpaired t-test, $t_{(8)}$=1.375, p=0.2110) and **E)** dopamine clearance rate (tau, Unpaired t-test, $t_{(8)}$=1.349, p=0.2141) indicating no significant differences. **F)** Phasic stimulation (5 pulses at 5, 10 and 20 Hz) current versus time plots (top) and color plots (bottom) showing enhanced dopamine release in response to increasing frequency of five pulse stimulations. **G)** Summary of dopamine release in response to phasic stimulation in GPR83 KO mice compared to WT (Two-way ANOVA Interaction F(3,24)= 1.175, p=0.3399, Frequency F(3,24)=22.2, ***p<0.0001, Genotype F(1,8)=9.098, **p<0.01, Holm-Sidak's multiple comparisons test, *p<0.05, **p<0.01, n=4–6mice/gp). **H**) Current versus time plots of

dopamine release represented as a percent of one pulse (tonic) release. **I)** Summary of normalized dopamine 27 release in response to phasic stimulation showing that the percent increase in dopamine release issignificantly blocked in GPR83 KO mice compared to WT. (Two-way ANOVA Interaction $F(2,18)= 6.460$, ** $p<0.01$, Frequency $F(2,18)=26.27$, *** $p<0.0001$, Genotype $F(1,9)=4.046$, $p=0.751$,n=4–6 mice/gr). **J)** Dopamine release measured before and after treatment with nicotinic acetylcholine receptor antagonist mecamylamine (2μM, MEC) in GPR83 WT (red) and GPR83 KO (blue). Data are represented as percent 1 pulse stimulation. (**WT**; Two-way ANOVA Interaction $F(5,48)= 2.44$, * $p<0.05$, MEC $F(1,48)=5.41$,*$p<0.05$, Frequency $F(5,48)=5.48$, *** $p<0.001$, **KO**; Two-way ANOVA Interaction $F(5,30)= 10.41$, *** $p<0.0001$, MEC $F(1,30)=2.51$,$p=0.1645$, Frequency $F(5,30)=11.39$, *** $p<0.001$, Bonferroni post-hoc analysis, *$p<0.05$, ** $p<0.01$, n=4–5 mice/gr). The data represents mean ± SEM.

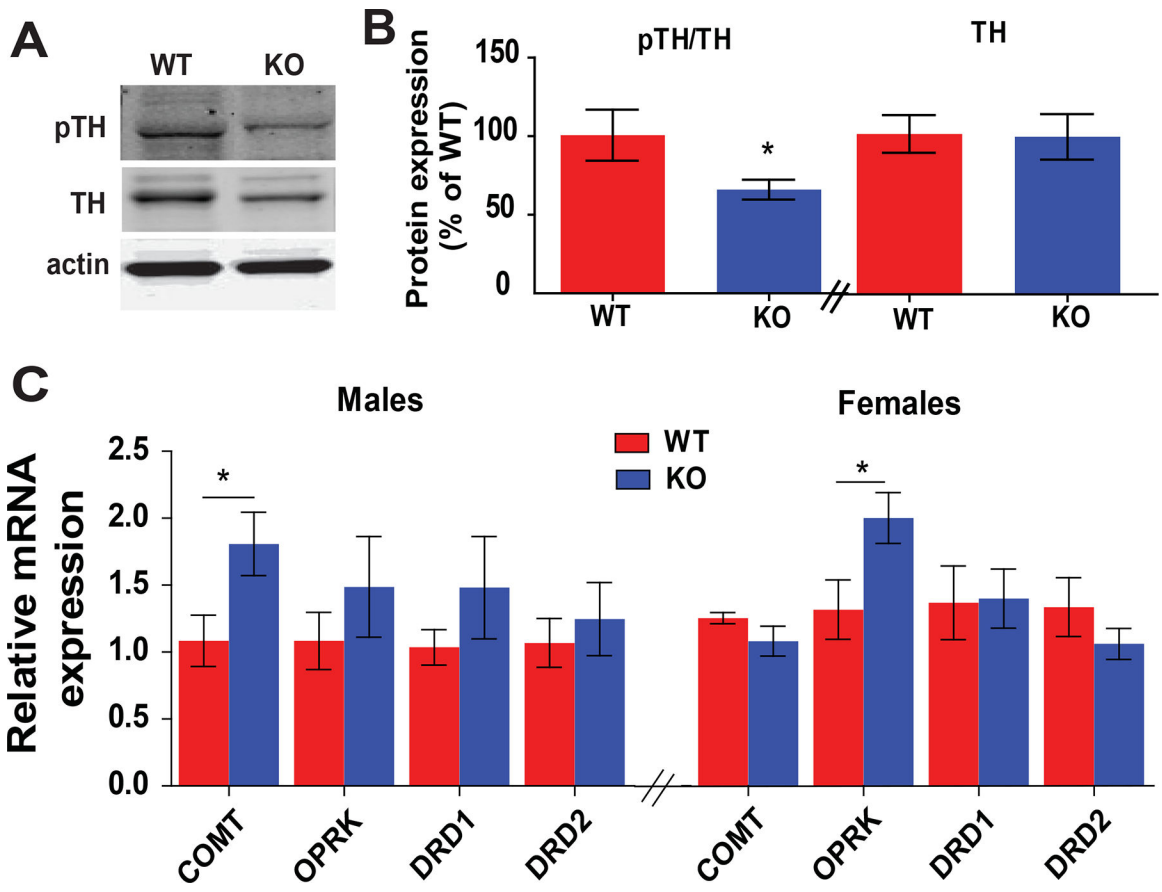

Figure 5: Analysis of dopamine related proteins in GPR83 KO mice.

VTA punches from GPR83 WT and KO mice were used to determine phosphorylation of tyrosine hydroxylase (TH). **A)** Western blot images of TH and pS40 pTH in the VTA of GPR83 WT and KO mice. **B)** Summary graphs of pTH (left) and total TH levels (right) in GPR83 WT versus KO mice (Unpaired t-test, pTH/TH, *$p<0.05$, $t_{(10)}=2.64$, n=8–9mice/gr; TH/actin $t_{(10)}=0.09794$, n=5–6 mice/gr). **C)** qPCR analysis of dopamine related proteins in the NAc of male and female GPR83 KO mice compared to WT. qPCR data are normalized to GPR83 WT (Unpaired t-tests, see Supplemental Table 2 for details, *$p<0.05$, n-=4–5 mice/gr). The data represents mean ± SEM.

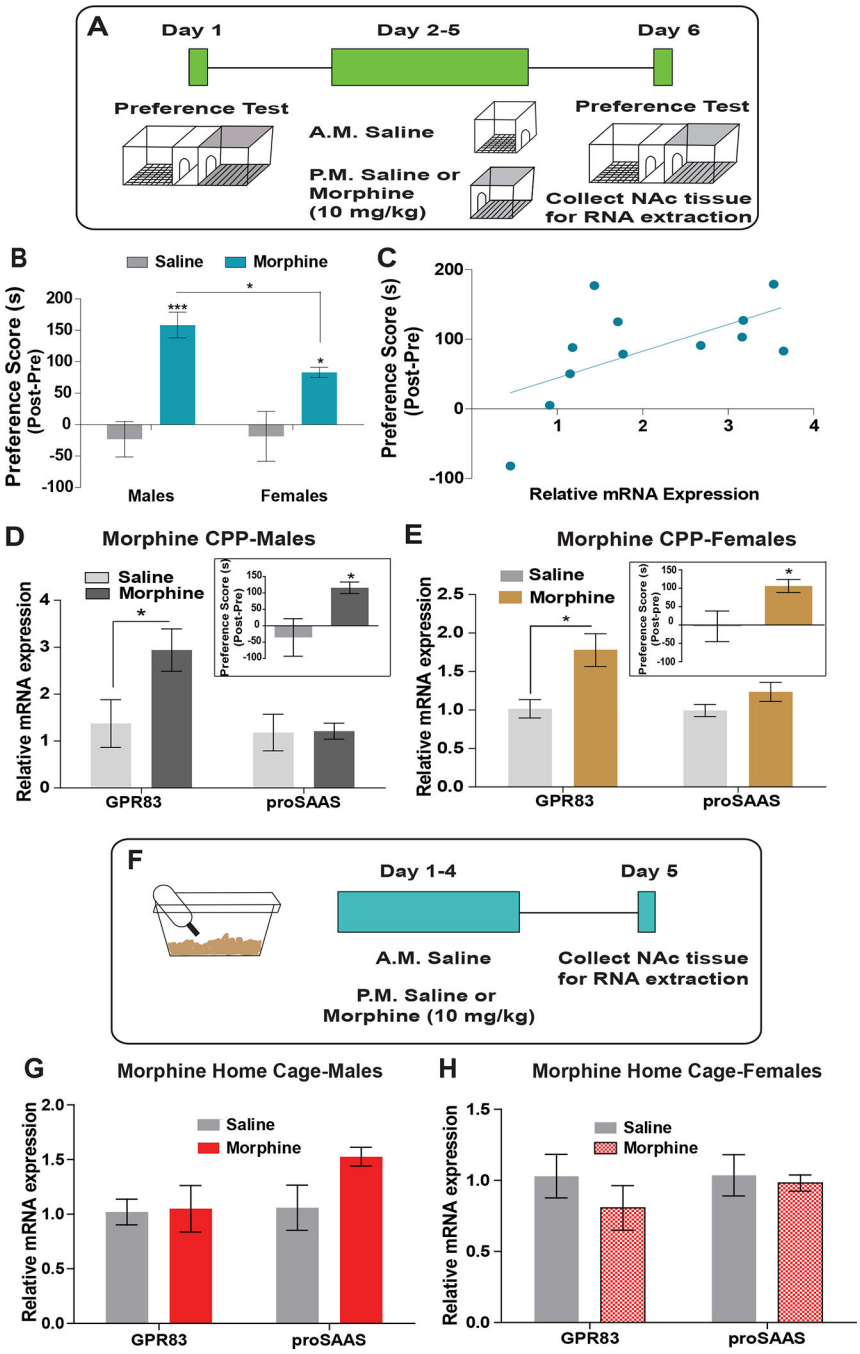

Figure 6: Regulation of GPR83 expression by morphine reward-learning.

A) Schematic of experimental design for morphine CPP (10mg/kg, i.p.; 4 consecutive days) and collection of tissue for qPCR analysis of GPR83 and proSAAS. **B)** In male and female mice, morphine CPP results in preference for the morphine paired chamber compared to saline controls. Females have a lower preference than male mice. (Two-way ANOVA Interaction $F(1,90)= 3.42$, $p=0.0675$, Morphine $F(1,90)=38.98$,***$p<0.0001$, Sex $F(1,90)=1.98$, $p=0.1631$, Bonferroni post-hoc analysis, *$p<0.05$, ***$p<0.0001$, n= 8–29 mice saline groups, n=24–36 mice morphine groups). **C)** Correlation analysis of GPR83

expression in the NAc and morphine preference score (r=0.3572; p=0.04, n=12 mice). **D and E)** A select group of male and female mice exposed to morphine CPP with similar morphine paired scores (inset; average males 116±17.5s, n=5; Average females 106.2±43.69 s, n= 6). (Males: Unpaired t-test *p<0.05, $t_{(8)}$=2.523, n=5/gr; Females: Unpaired t-test *p<0.05, $t_{(11)}$=2.85, n=6–7/gr). Morphine CPP increases expression of GPR83 but not proSAAS in the NAc in both male and female mice. (Unpaired t-test, *p<0.05, GPR83, $t_{(6)}$=2.312, proSAAS, $t_{(7)}$=0.081, n=4–5 mice/gr; Females: Unpaired t-test, GPR83 *p<0.05, $t_{(10)}$=2.91, proSAAS, p=0.11, $t_{(10)}$=1.74, n=6 mice/gr). **F)** Schematic of experimental design for morphine home cage treatment and collection of tissue for qPCR analysis of GPR83 and proSAAS. **G and H)** Morphine administered in the home cage (same dose and schedule) does not increase expression of GPR83 or proSAAS in the NAc of male or female mice. (Males: Unpaired t-test, GPR83, p=0.91, $t_{(7)}$=0.123, proSAAS, p=0.082 $t_{(6)}$=2.088, n=4 mice/gr; Females: Unpaired t-test, GPR83, p=0.35, $t_{(6)}$=1.01, proSAAS, p=0.74, $t_{(6)}$=0.35, n=4 mice/gr). The data represents mean ± SEM.

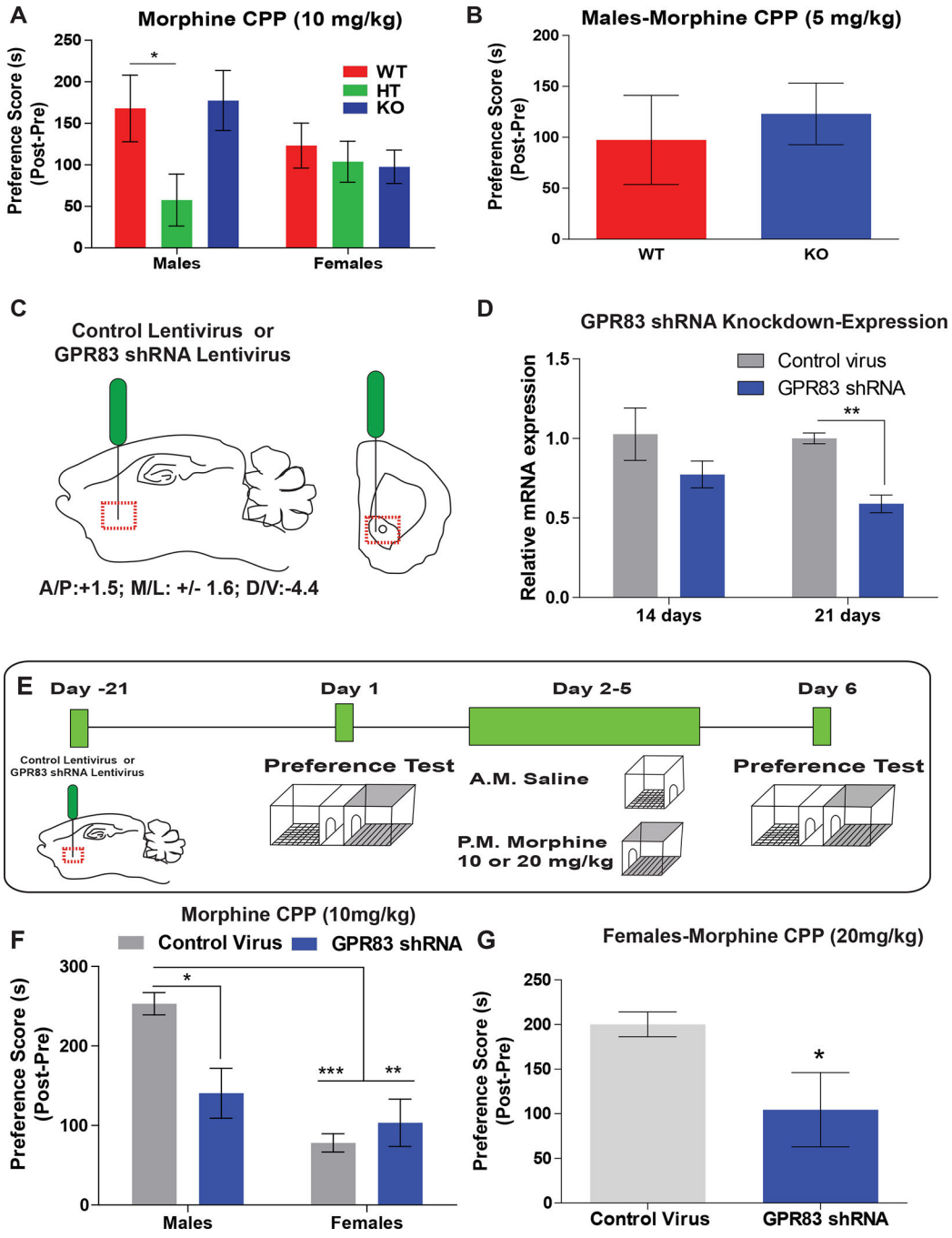

Figure 7: The effect of GPR83 knockout and knockdown in the NAc on morphine reward.

A) Morphine CPP (10 mg/kg) in male and female GPR83 WT, HT and KO mice. (Two-way ANOVA Interaction F(2,51)= 1.93, p=0.1550, Genotype F(2,51)=2.38, p=0.1032, Sex F(1,51)=0.94, p=0.3377, Bonferroni post-hoc analysis, *p<0.05, n= 7–12 mice/gr. **B)** Morphine CPP (5 mg/kg) in male GPR83 WT and KO mice. **(**Unpaired t-test, p=0.6315, $t_{(21)}$=0.4868, n=11–12 mice/gr. **C)**Schematic of control and GPR83 shRNA lentiviral injections into the NAc of male and female mice. **C)** Two and three weeks later punches of NAc were collected for qPCR analysis (Twoway ANOVA, Interaction F(1,8)=0.65, p=0.44;

GPR83 KD F(1,8)= 11.46, p<0.01; Time F(1,8)=1.15, p=0.32; Bonferroni post-hoc tests, Control Virus vs GPR83 shRNA, at 21 days, p<0.05, n=3/gr). **C)** Schematic of experiments using lentiviral knockdown of GPR83 in the NAc followed by morphine CPP training. **D)** Knockdown of GPR83 in the NAc decreases morphine preference in male but not female mice using a 10 mg/kg dose (Two-way ANOVA, Interaction, F(1,25)=8.16, p<0.01, GPR83 shRNA, F(1,25)=3.28, p=0.08, Sex F(1,25)=19.32, p<0.0001; Bonferroni post-hoc tests Control virus vs GPR83 shRNA males **p<0.01, n=6–8 mice/gr). **E)** In female mice morphine CPP using a 20 mg/kg dose results in a higher preference than the 10 mg/kg dose; this is attenuated by GPR83 knockdown in the NAc. Unpaired t-test *p<0.05, t=2.414, df=14, n=7–9/gp. The data represents mean ± SEM.